Title	Mechanism of strong affinity of clay minerals to radioactive cesium; First-principles calculation study for adsorption of cesium at frayed edge sites in muscovite
Author(s)	Masahiko OKUMURA , Hiroki NAKAMURA, Masahiko MACHIDA
Citation	Journal of the Physical Society of Japan,82(2) ; p.033802
Text Version	Author
URL	http://jolissrch-inter.tokai-sc.jaea.go.jp/search/servlet/search?5039766
DOI	http://dx.doi.org/10.7566/JPSJ.82.033802
Right	© 2013 The Physical Society of Japan

Mechanism of Strong Affinity of Clay Minerals to Radioactive Cesium: First-Principles Calculation Study for Adsorption of Cesium at Frayed Edge Sites in Muscovite

Masahiko Okumura*, Hiroki Nakamura, and Masahiko Machida

CCSE, Japan Atomic Energy Agency, Kashiwa, Chiba 277–8587, Japan

The present first-principles study based on density-functional theory confirms that frayed edge sites (FESs) formed in micaceous clays have a crucial role in the long-term stability of radioisotopes of Cs on the topsoil surface. An FES is modeled according to the weathering scenario of muscovite, and the substitution of originally occupied K with Cs is virtually simulated. The calculation results clearly demonstrate that such a replacement is strongly promoted only when the stack structure is loosely expanded at the clay edges. This is the first atomic-scale confirmation of the strong affinity of FESs to Cs, which may shed new light on the decontamination engineering of soil materials.

KEYWORDS: frayed edge, muscovite, clay mineral, radioactive cesium, density functional theory

Clay is one of the most widely abundant materials on the earth.[1] Their physicochemical properties are so rich that humans cleverly utilize their flexible plasticity, annealing sinterability, ion-exchange ability, water expansibility, etc., in daily life as well as in industry. Among their various useful features, the ion-exchange ability is of great importance, since soil retains several essential minerals including potassium, calcium, and magnesium for plants and other organisms to feed and grow. In this paper, we study a typical characteristic of clays, i.e., the retention mechanism of a specific mineral, Cs, in spite of its lack of use by living creatures.

A trace amount of Cs is well known to be strongly adsorbed by clay materials.[2–4] So far, the reason for this has been puzzling. From the 1950s to 1980s, the global fallout from atmospheric nuclear weapon testing[5] and the release of large amounts of radionuclides by the Chernobyl nuclear power plant accident[6] caused the worldwide deposition of radioactive Cs on topsoil.[7,8] The fallout radioisotopes of Cs have continued to remain on the top surface for a long time even to the present day. The radioisotopes of Cs released from the Fukushima Dai-ichi nuclear power plant accident[9,10] also exhibit the above notable characteristic.[11]

The adsorption of radioactive Cs by clay minerals has been mainly studied by experimental ways. Consequently, mica, a type of 2:1 phyllosilicate, is well known to tightly adsorb Cs by the substitution of an interlayer cation with Cs.[2–4] Figure 1 schematically displays the crystalline structure of mica, in which the 2:1 unit layer comprises an octahedral sheet sandwiched by two tetrahedral sheets and the 2:1 layers are bounded by cations, resulting in a periodic stacked structure along the c-axis. The central elements of the tetrahedron and octahedron are silicon and aluminum, respectively, and silicon is partly substituted with aluminum. Thus, the substituted tetrahedron is negatively charged, requiring cations to compensate the emerging charges. An example of the substitution is displayed in the bottom-left panel of Fig. 1, where K ions slip into the interlayer sites and stabilize the mica structure. Octohedral sheets are classified into two types: dioctahedral sheets constructed from trivalent cations, Al^{3+} or Fe^{3+}, and trioctahedral sheets made of divalent cations, Mg^{2+} or Fe^{2+}.

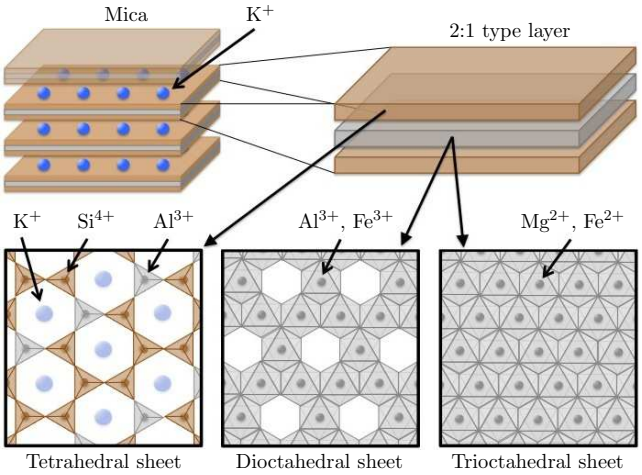

Fig. 1. (Color online) Schematic structure of 2:1 phyllosilicates.

So far, some experimental measurements have revealed that mica has three types of adsorption sites for Cs.[12,13] They are called types I, Ⅱ, and Ⅲ. Among these three types, the type I and Ⅱ sites show low cation exchange capacity compared with that of type Ⅲ, while their selectivity and retention stability for Cs is quite high compared with these of type Ⅲ. Moreover, the populations of the type I and Ⅱ sites are considerably smaller than that of the type Ⅲ site. These peculiarities of types I and Ⅱ have led to widespread acceptance of the fact that a trace amount of radioactive Cs is selectively and irreversibly adsorbed in mica, while the adsorbed Cs becomes exchangeable only when its amount is large. Indeed, several experiments testing the elution characteristics of radioactive Cs in Fukushima natural soils demonstrate that most of the trace amount of Cs cannot be changed into a soluble form.[14] Thus, the roles of the type I and Ⅱ sites are of great importance for the volume reduction of waste materials left over from decontamination processes. In this paper, we concentrate on the type I and Ⅱ sites in mica.

Figure 2(a) schematically displays the proposed adsorption sites in mica[4,13] at the atomic scale. These sites are classi-

*E-mail address: okumura.masahiko@jaea.go.jp

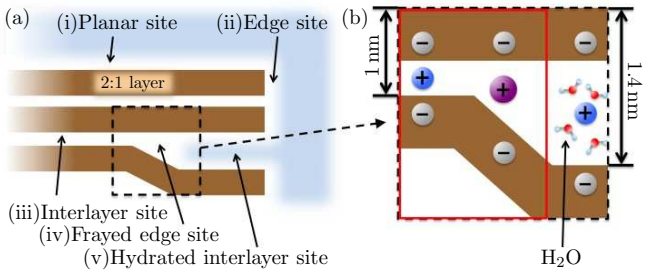

Fig. 2. (Color online) (a) Adsorption sites in micaceous minerals. (b) Structure of a frayed edge site.

fied into (i) planar, (ii) edge, (iii) interlayer, (iv) frayed edge, and (v) hydrated interlayer sites depending on their locations. Among them, the frayed edge site (FES) and hydrated interlayer site are regarded as being related to disordered structure formed by weathering as shown in Fig. 2. These sites are composed of three regions, one of which is characterized by the normal muscovite structure whose interlayer distance is about 1 nm, another of which is considered to be partly expanded by the insertion of cations accompanying water molecules, resulting in the interlayer expansion to about 1.4 nm, and the other of which is a wedge-shaped region between the above two regions as shown in Fig. 2(b).[4)] The atomic scale structure of the type I and Ⅱ sites was suggested to be related to the FES,[12,13)] while the type Ⅲ site is considered to be ubiquitously spread on nonspecific edges and wide planar surfaces whose affinity to Cs is not selective and irreversible.[12,13)] These ideas are based on the results of batch experiments, although no direct atomic scale confirmation has been reported.

On the basis of the FES image in Fig. 2(b), an index to estimate the quantity of radioisotopes of Cs adsorbed by FESs per unit soil volume has been suggested. It is called the "radiocesium interception potential" (RIP),[15,16)] whose value can be obtained by covering all other sites with sufficiently dense AgTU or Ca^{2+} and measuring the selectivity of radioactive Cs for K on the uncovered FESs. The RIP value is known to be about 0.006 mol/kg in kaolinite, one of the 1:1 phyllosilicates, while that in mica reaches 11.8 mol/kg, indicating the strong and selective affinities of Cs to FESs.[17)] Indeed, scanning electron microscopy and X-ray microprobe measurements roughly confirmed that radioactive Cs is fixed only around the edge of micas. These results strongly support the selective affinity for Cs of FESs.[18)]

As schematically shown in Fig. 2, FESs correspond to local structural distortions inside a clay grain. The direct atomic scale confirmation is too difficult for current experimental techniques owing to their fine atomic scale and rare structure. On the other hand, computational methods to explore atomic scale physics are promising alternatives, for which numerical techniques have been fully developed in the last decade together with the rapid invention of hardware. In particular, density functional theory (DFT)[19,20)] and molecular dynamics have been frequently employed for clay minerals.[21–27)] However, no direct work toward clarifying the mechanism of the strong affinity of Cs in FESs has been published yet. In this paper, we employ a first-principles calculation scheme based on DFT and microscopically examine the strong selective affinity of FES to Cs.

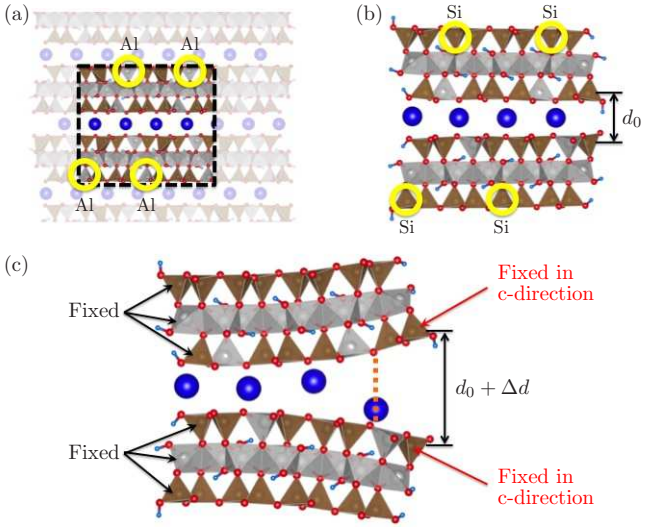

Fig. 3. (Color online) Model of FES employed in this paper. The yellow circles stand for the positions of Al replaced by Si in the present separated FES model. The orange dotted line indicates the location of the energy surface plane depicted in Fig. 5.

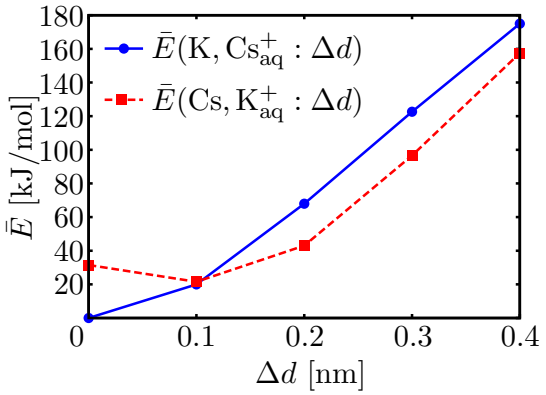

Fig. 4. (Color online) $\bar{E}(\mathrm{A}, \mathrm{B}^+_{\mathrm{aq}} : \Delta d)$ versus Δd. For the definitions of $\bar{E}$ and Δd, see the text.

Now, let us present the simulation scheme and modeling. The simulation target is an atomic-scale unresolved structure requiring DFT-based analysis. Note that the number of atoms in DFT is restricted to within a few hundred atoms owing to computational resource limitations. Then, we create a model of an FES and carry out analysis using the model. The employed calculation program is the Vienna Ab initio Simulation Package (VASP),[28,29)] which supports the projected augmented wave method[30,31)] and generalized gradient approximation,[32)] which are also employed in this work similar to several previous works on clays.[25,26)] The cutoff energy is 1600 eV, and 3×1×1 sampling points are used on k-point grids. Structural relaxation is repeated until the gradient forces on atoms are less than 2.0×10^{-2} eV/Å.

The modeling of the FES is as follows. i) First, we obtain the ground state of the bulk mica and select a part of it to make an edge as shown in Fig. 3(a). The distribution of substituted Al atoms in the bulk system follows that in ref.[26)] (see the left-bottom panel in Fig. 1 and the left panel of Fig. 2 in ref.[26)]). To maintain the charge neutrality of the separated system, we

substitute Al with Si on the outer tetrahedral sheets, shown by yellow circles in Figs. 3(a) and 3(b), and also attach H onto O at the cut edges. ii) Al and Si atoms at the left-hand edge are fixed to maintain an interlayer distance of approximately 1 nm, as shown in Fig. 3(c), and the atoms at the opposite edge are gradually shifted to expand the interlayer distance to $\sim$ 1.4 nm ($\Delta d \sim 0.4$ nm). After each stepwise shift, the structural relaxation is always executed, and subsequently the outermost K is virtually replaced by Cs in every shift step. The energies before and after the replacement, respectively defined as $E(\mathrm{K} : \Delta d)$ and $E(\mathrm{Cs} : \Delta d)$, are calculated for each shift. In addition to the energies, the hydration energies for K and Cs, expressed as $E(\mathrm{K}^+_{\mathrm{aq}})$ and $E(\mathrm{Cs}^+_{\mathrm{aq}})$, respectively, are taken into account, and the energies before and after the ion exchange with water molecules are calculated as

$$E(\mathrm{K}, \mathrm{Cs}^+_{\mathrm{aq}} : \Delta d) = E(\mathrm{K} : \Delta d) + E(\mathrm{Cs}^+_{\mathrm{aq}}) , \quad (1)$$

$$E(\mathrm{Cs}, \mathrm{K}^+_{\mathrm{aq}} : \Delta d) = E(\mathrm{Cs} : \Delta d) + E(\mathrm{K}^+_{\mathrm{aq}}) . \quad (2)$$

Here, we employ the experimental value[33] for each hydration energy $E(\mathrm{K}^+_{\mathrm{aq}})/E(\mathrm{Cs}^+_{\mathrm{aq}})$ according to ref.[25] Setting the energy bottom at $E(\mathrm{K}, \mathrm{Cs}^+_{\mathrm{aq}} : \Delta d = 0)$, we introduce the energy value from the energy bottom, $\bar{E}(\mathrm{Cs}, \mathrm{K}^+_{\mathrm{aq}} : \Delta d)$, as

$$\bar{E}(\mathrm{A}, \mathrm{B}^+_{\mathrm{aq}} : \Delta d) = E(\mathrm{A}, \mathrm{B}^+_{\mathrm{aq}} : \Delta d) - E(\mathrm{K}, \mathrm{Cs}^+_{\mathrm{aq}} : \Delta d = 0) , \quad (3)$$

where A and B represent the cations involved in the exchange.

Now, let us present the calculation results. One easily finds that $\bar{E}(\mathrm{K}, \mathrm{Cs}^+_{\mathrm{aq}} : \Delta d = 0) < \bar{E}(\mathrm{Cs}, \mathrm{K}^+_{\mathrm{aq}} : \Delta d = 0)$ and that $\bar{E}(\mathrm{K}, \mathrm{Cs}^+_{\mathrm{aq}} : \Delta d = 0)$ is never larger than $\bar{E}(\mathrm{Cs}, \mathrm{K}^+_{\mathrm{aq}} : \Delta d = 0)$ until $\Delta d \sim 0.1$. These results indicate that the substitution of K with Cs is energetically unfavorable in the non-frayed edges of mica, i.e., mica does not naturally adsorb Cs if not all of the edges are expanded. This is consistent with the results of virtual equivalent replacement in the bulk periodic system reported in ref.[25] These findings clearly suggest the importance of frayed structures emerging at surfaces and edges for Cs replacement.

Next, we examine the frayed cases by increasing Δd. Figure 4 shows the inversion between $\bar{E}(\mathrm{K}, \mathrm{Cs}^+_{\mathrm{aq}} : \Delta d)$ and $\bar{E}(\mathrm{Cs}, \mathrm{K}^+_{\mathrm{aq}} : \Delta d)$, which indicates that the ion exchange of K with Cs naturally tends to occur at the FES. Namely, a free Cs ion can be fixed at an FES together with the release of K when the interlayer distance is increased to more than $\Delta d \sim 0.1$ nm. If such expanded FESs still retaining K exist on mica grains, then the ion exchange naturally occurs when radioisotopes of Cs accidentally come into the area. The result in Fig. 4 strongly supports the scenario of the high affinity of FESs to Cs. Although the FES scenario has been widely accepted by nuclear waste management scientists and engineers as well as geologists and agriculturists, there has so far been no atomic-scale confirmation of the scenario. We believe that the present DFT result is the first scientific confirmation of the scenario.

Here, we discuss the reason why FES has such strong affinity for Cs. We compare the cases of $\Delta d = 0$ and $\Delta d = 0.3$ nm, because the former is simply the non-frayed case while the latter exhibits the largest energy difference upon the exchange with Cs as shown in Fig. 4. In order to clarify the inner spheres of the cations adsorbed at FESs, we examine the energy surfaces on a fixed slice whose location is indicated by the orange dotted line shown in Fig. 3(c). We move the adsorbed cation inside the slice plane perpendicular to Fig. 3(c) and calculate the $\boldsymbol{r}$-dependent energy, defined as

$$\bar{E}(\boldsymbol{r} : \mathrm{A}, \mathrm{B}^+_{\mathrm{aq}} : \Delta d) = E(\boldsymbol{r} : \mathrm{A}, \mathrm{B}^+_{\mathrm{aq}} : \Delta d) - E(\mathrm{K}, \mathrm{Cs}^+_{\mathrm{aq}} : \Delta d = 0) , \quad (4)$$

where A and B are K and Cs or Cs and K, respectively. Figures 5(a) and 5(b) exhibit the calculated energy surface for each cation when $\Delta d = 0$. One easily finds that the energy well for K is deeper than that for Cs although both minimum points are located at the center between the 2:1 layers. In contrast, when $\Delta d = 0.3$ nm, the surfaces drastically change, as shown in Figs. 5(c) and 5(d). The minimum value for K is higher than that for Cs, as shown in Fig. 5(c), and the minimum positions of K and Cs are different as shown in Figs. 5(c) and 5(d).

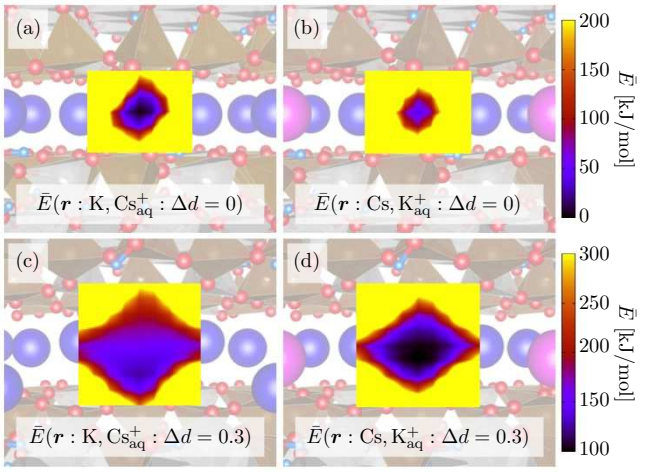

Fig. 5. (Color online) $\bar{E}(\boldsymbol{r} : \mathrm{A}, \mathrm{B}^+_{\mathrm{aq}} : \Delta d)$ for (a) A = K and B = Cs when $\Delta d = 0$, (b) A = Cs and B = K when $\Delta d = 0$, (c) A = K and B = Cs when $\Delta d = 0.3$ nm, and (d) A = Cs and B = K when $\Delta d = 0.3$ nm. The definition of $\bar{E}(\boldsymbol{r} : \mathrm{A}, \mathrm{B}^+_{\mathrm{aq}} : \Delta d)$ is given in the text.

These results ($\Delta d = 0.3$ nm) can be explained as follows. Firstly, the negatively charged tetrahedral layers attract a cation, as shown in Figs. 6(b), 6(e), 7(b), and 7(e). Since the electrostatic attraction acts on the cation from both the upper and lower layers, the potential minimum becomes deepest when the energy potentials from the upper and lower layers overlap. Such a superimposed situation occurs for K at $\Delta d \sim 0$ [Fig. 6(c)], while the same situation occurs for Cs at $\Delta d \sim 0.3$ nm [Fig. 7(f)]. On the other hand, the nonsuperimposed situation occurs for Cs at $\Delta d = 0$, as shown in Fig. 6(f), and for K at $\Delta d = 0.3$ nm, as shown in Fig. 7(c). The origin of the difference in the energy potential shapes for K and Cs is the cation radius. The distance of the minimum point of the Lennard–Jones type potential from the sheet surface becomes larger as the cation radius increases. This is why the conditions for the superimposed situation are different for K and Cs. In terms of the above simple analysis based on the ion radius, it should be mentioned that the energy surface for K shown in Fig. 5(c) actually has a single minimum, although the corresponding situation shown in Fig. 7(c) has multiple minima. This is because of the position of K next to the outermost K at the edge. As shown in Fig. 7(a), the neighboring K drifts from the center between two 2:1 layers when Δd is increased from 0. This is because the replacement of Si by Al occurs in an imbalanced manner in the upper and lower sheets as

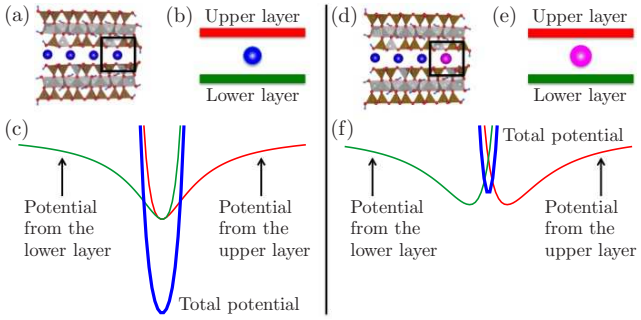

Fig. 6. (Color online) Structure of FES model before expanding the edge ($\Delta d = 0$) with (a) K and (d) Cs at the edge. Schematic configuration of negatively charged 2:1 layer with (b) K and (e) Cs. Total potential and superposition of potentials from the layers to (c) K and (f) Cs.

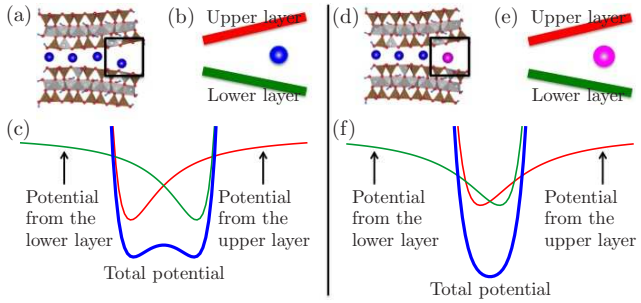

Fig. 7. (Color online) Structure of FES model after expanding the edge ($\Delta d = 0.3$ nm) with (a) K and (d) Cs at the edge. Schematic configuration of negatively charged 2:1 layer with (b) K and (e) Cs. Total potential and superposition of potentials from the layers to (c) K and (f) Cs.

shown in Fig. 3. Then, the upwardly shifted K screens the upper sheet charge and weakens the force from the upper sheet. This makes the energy surface on the slice deviate from the expected simple situation as shown in Fig. 7(c). From these results, it is found that the exchange energy at an FES also varies with the chemical characteristics of both sheets.

From the above discussion, it is found that weathered mica clearly supplies strong retention sites for radioisotopes of Cs. Then, the next important issue is how to extract radioisotopes of Cs from FES. A physically possible scheme is simply to induce further weathering, i.e., further increase the interlayer distance, which enables the substitution of Cs with other elements or molecules having a larger radius than Cs. In contrast, possible chemical scheme is to cut the stabilized bonds between the mica 2:1 sheets and Cs. An effective way to achieve this is to use acids to induce protonation of the mica 2:1 layer and subsequently erosion of Al, Si, and Cs. Although the effectiveness of this chemical scheme has been experimentally confirmed, the damage to soils has to be minimized. The issue still remains unsolved. Further studies are required to establish the best way to remove Cs.

Finally, we note that the present calculations employ the experimental value of the cation hydration energy as ref.[25] This hydration energy is given in "bulk" water. This simplification is useful for clarifying the mechanism of Cs exchange in FES. However, we can improve the evaluation by modeling the situation in a more realistic manner. For example, if one can simulate the dynamics of both the cations and water molecules at the hydrated interlayer site, the exchange energy, Cs selectivity of FESs, etc., will be directly accessible. In addition, to complete the analysis in this paper, the exchange energy dependence on substitution patterns in the tetrahedral sheet should be evaluated. These advanced issues will be reported elsewhere.

In conclusion, we performed first-principles calculations in order to clarify why FES adsorbs and strongly retain a trace amount of radioactive Cs. Using the FES model based on the weathering scenario, the interlayer distance at one side of a crystalline edge was gradually expanded, and the substitution of K with Cs was simulated while measuring the energy difference. We found that the sign of the energy difference obtained by the exchange is inverted from positive to negative above a constant expansion distance, and the inversion mechanism is attributed to the cation-radius dependent superimposed effect of electrostatic potentials from upper and lower layers. In addition, we discussed some methods of removing Cs from FESs on the basis of the mechanism.

We would like to acknowledge K. Kawamura, Y. Ohnishi, Z. Yoshida, T. Ohnuki, and K. Muramatsu for their useful discussions. All calculations were done on a BX900 supercomputer in CCSE, JAEA. We thank the director of CCSE, M. Tani, and all other staff members In addition, we thank A. Fujiwara and K. Mori for their computational technical advice, and M.M. is indebted to A. Nakao for his illuminating discussion of FESs. This work was partially supported by JAEA-NIMS cooperative project organized by T. Yaita. We thank all the project members for their useful discussion. The figures shown in Figs. 3(a)–3(c), 6(a), 6(d), 7(a), and 7(d) were drawn using VESTA.[34]

1) R. H. Grim: *Clay Mineralogy* (McGraw-Hill, New York, 1968) 2nd ed.
2) B. L. Sawhney: Clays Clay Miner. **20** (1972) 93.
3) R. M. Cornell: J. Radioanal. Nuclear Chem. **171** (1993) 483.
4) B. Delvaux, N. Kruyts, E. Maes, and E. Smolders: in *Trace Elements in the Rhizosphere*, ed. G.R. Gobran, W.W. Wenzel, and E. Lombi (CRC Press, Florida, 2001) p. 61.
5) United Nations Scientific Committee on the Effects of Atomic Radiation: *United Nations Scientific Committee on the Effects of Atomic Radiation 2000 Report to the General Assembly with Scientific Annexes, Volume I: SOURCES* (United Nations Publications, New York, 2000).
6) International Atomic Energy Agency: *Summary Report on the Post-accident Review Meeting on the Chernobyl Accident* (International Atomic Energy Agency, Vienna, 1986).
7) M. Komamura, A. Tsumura, N. Yamaguchi, N. Kihou, and K. Kodaira: Misc. Publ. Natl. Inst. Agro-Environ. Sci. **28** (2005) 1.
8) K. Hirose, Y. Igarashi, and M. Aoyama: Appl. Radiat. Isot. **66** (2008) 1675.
9) Prime Minister of Japan and His Cabinet: *Report of Japanese Government to the IAEA Ministerial Conference on Nuclear Safety– The Accident at TEPCO's Fukushima Nuclear Power Stations–*, http://www.kantei.go.jp/foreign/kan/topics/201106/iaea_houkokusho_e.html (2011).
10) Ministry of Education, Culture, Sports, Science and Technology: *Monitoring Information of Environmental Radioactivity Level*, http://radioactivity.mext.go.jp/en/ (2012).
11) H. Kato, Y. Onda, and M. Teramage: J. Environ. Radioact. **111**, (2012) 59.
12) E. Brouwer, B. Baeyens, A. Maes, and A. Cremers: J. Phys. Chem. **87** (1983) 1213.
13) R. N. J. Comans, M. Haller, and P. De Preter: Geochim. Cosmochim. Acta **55** (1991) 433.
14) N. Kozai, T. Ohnuki, M. Arisaka, M. Watanabe, F. Sakamoto, S. Ya-

masaki, and M. Jiang: J. Nucl. Sci. Technol. **49** (2012) 473.
15) A. Cremers, A. Elsen, P. De Peter, and A. Maes: Nature **335** (1988) 247.
16) J. Wauters, A. Elsen, A. Cremers, A. V. Konoplev, and A.A. Bulgakov: Appl. Geochem. **11** (1996) 589.
17) A. Nakao, Y. Thiry, S. Funakawa, and T. Kosaki: Soil Sci. Plant Nutr. **54** (2008) 479.
18) J. P. McKinley, J. M. Zachara, S. M. Heald, A. Dohnalkova, M. G. Newville, and S. R. Sutton: Environ. Sci. Technol. **38** (2004) 1017.
19) P. Hohenberg and W. Kohn: Phys. Rev. **136** (1964) B864.
20) W. Kohn and L. J. Sham: Phys. Rev. **140** (1965) A1133.
21) R. T. Cygan, J.-J. Liang, and A. G. Kalinichev: J. Phys. Chem. B **108** (2004) 1255.
22) J. L. Suter, R. L. Anderson, H. C. Greenwell, and P. V. Coveney: J. Mater. Chem. **19** (2009) 2482.
23) H. Sakuma and K. Kawamura: Geochim. Cosmochim. Acta **75** (2011) 63.
24) M. C. Pitman and C.T. van Duin: J. Am. Chem. Soc. **134** (2012) 3042.
25) K. M. Rosso, J. R. Rustad, and E. J. Bylaska: Clays Clay Miner. **49** (2001) 500.
26) B. Militzer, H.-R. Wenk, S. Stackhouse, and L. Stixrude: Am. Mineral. **96** (2011) 125.
27) S. Suehara, H. Yamada, and T. Sasaki: Phys. Rev. B **85** (2012) 224203.
28) G. Kresse and J. Hafner: Phys. Rev. B **47** (1993) 558.
29) G. Kresse and J. Furthmüller: Phys. Rev. B **54** (1996) 11169.
30) P.E. Bloch: Phys. Rev. B **50** (1994) 17953.
31) G. Kresse and D. Joubert: Phys. Rev. B **59** (1999) 1758.
32) J.P. Perdew, K. Burke, and M. Ernzerhof: Phys. Rev. Lett. **77** (1996) 3865.
33) D. R. Lide ed., *CRC Handbook of Chemistry and Physics*, 90th edition (CRC Press, Boca Raton, 2009).
34) K. Momma and F. Izumi: J. Appl. Crystallogr. **44** (2011) 1272.